^{75}As NMR study of oriented CeFeAsO and $CeFeAsO_{0.84}F_{0.16}$

A. Ghoshray,* B. Pahari, M. Majumder, M. Ghosh, K. Ghoshray, B. Bandyopadhyay, P. Dasgupta, A. Poddar, and C. Mazumdar

ECMP Division, Saha Institute of Nuclear Physics, 1/AF Bidhannagar, Kolkata-700064, India

(Received 18 January 2009; published 15 April 2009)

We report the resistivity and ^{75}As nuclear magnetic resonance (NMR) results of superconducting $CeFeAsO_{0.84}F_{0.16}$ and its parent compound CeFeAsO. The derivative of the resistivity with temperature and ^{75}As NMR in CeFeAsO clearly show a signature of the onset of the long-range magnetic ordering. The resistivity in $CeFeAsO_{0.84}F_{0.16}$ drops sharply at 41 K and becomes zero at 38 K. Analyzing the ^{75}As NMR spectra in $CeFeAsO_{0.84}F_{0.16}$ and CeFeAsO, we obtained the value of quadrupolar splitting frequency ν_Q =11.0 and 9.9($\pm$0.2) MHz and asymmetry parameter η=0.09 and 0.02, respectively. The shift (K_{ab}) in the oriented ($H\|ab$) $CeFeAsO_{0.84}F_{0.16}$ sample starts to decrease from 60 K (above T_c). Below 30 K, the NMR line broadens asymmetrically due to the formation of vortex lattice and the observed NMR spectra at 4–10 K clearly resemble the Redfield pattern.

DOI: 10.1103/PhysRevB.79.144512 PACS number(s): 74.70.−b, 74.25.Qt, 76.60.Cq

I. INTRODUCTION

The discovery of superconductivity in the family of rare-earth quaternary oxypnictides with the general formula *Ln*FeAsO (*Ln*=La, Ce, Pr, Nd, Sm Gd, Tb, and Dy) (Refs. 1–8) is generating much excitement in the condensed-matter community. This is because of the emergence of superconductivity with transition temperatures as high as T_C =26–55 K under electron or hole doping of their nonsuperconducting parent compounds. Superconductivity with T_C =38 K has also been reported for $Ba_{1-2\delta}K_{2\delta}Fe_2As_2$ (Ref. 9) but $BaFe_2As_2$ is not superconducting. In all these systems, superconductivity arises when *Ln*-O and Ba charge reservoir layers donate superconducting carriers to the common FeAs layers forming edge-sharing $FeAs_4$ tetrahedra. These are reminiscent of the case of the high-T_C cuprates, where carrier doping from charge reservoir layers transforms the undoped Mott-insulating CuO_2 layers into superconducting $(CuO_2)^{-2+\delta}$, where δ is the carrier concentration. In this case, most of the properties appear to be related to the effects of strong electron correlations induced by the on site Coulomb repulsions among the electrons in the narrow Cu 3*d* band. On the other hand, for *Ln*FeAsO systems, the recent x-ray absorption and photoemission spectroscopy in the normal state of $CeFeAsO_{0.89}F_{0.11}$ exhibit signatures of Fe *d*-electron itinerancy.[10] Moreover, the exchange multiplets appearing in the Fe 3*s* core level indicate the presence of strong itinerant spin fluctuations; but it cannot explain the Ce-alone contribution to the Curie-Weiss susceptibility.

Furthermore, all the parent *Ln*FeAsO compounds exhibit similar anomaly in the resistivity in the range 145–150 K, which was initially ascribed to a spin-density wave (SDW)-type antiferromagnetic (AF) order. This anomaly has now been clarified from neutron[11] and x-ray scattering[12] measurements. It is established that this is due to a structural transition from tetragonal (space group: $P4/nmm$) to the monoclinic phase (*Cmma*). Nevertheless, in case of LaFeAsO, this study further reveals a SDW-type AF ordering at 140 K below the structural transition observed at 155 K. A two-peak structure observed in the heat-capacity measurement of the nondoped sample[13] confirmed this picture. The location of the high-temperature peak agrees with that of the crystallographic transition. Local probe techniques, e.g., ^{57}Fe Mossbauer spectroscopy[14] revealed a strong internal magnetic field that starts to appear at 140 K. ^{139}La-NMR measurements[15] also clarified the critical divergence of T_1 due to the AF ordering at 140 K. These results indicate that AF ordering occurs at 145 K, corresponding to the low-temperature heat-capacity peak. Similar two peaks (overlapping) in the heat-capacity measurements are observed in each case of CeFeAsO, PrFeAsO, and NdFeAsO.[16] This demonstrates the existence of the distinct structural and long-range magnetic ordering in the parent materials. Later on, it is also confirmed from neutron scattering[17,18] that the magnetic transition is due to the SDW-type AF ordering of the small moments of iron [e.g., $0.8\mu_B$ for CeFeAsO,[19] $0.48\mu_B$ for PrFeAsO,[17] and $0.25\mu_B$ for NdFeAsO (Ref. 20)]. The rare-earth moments also undergo an AF ordering in the temperature range 4–14 K. With fluorine doping (x=0.06), Fe ordering temperature shifts from 140 to 10 K, whereas, the effect on the Ln ordering temperature is considerably less.[19] For example, for the Ce moment in CeFeAsO exhibit AF ordering at 3.7 K and the 16% F-doped sample also shows the onset signature of AFM ordering down to 1.8 K[2].

In this paper, we provide a microscopic look at the local electronic properties of $CeFeAsO_{1-x}F_x$ using ^{75}As nuclear magnetic resonance (NMR) in grain-aligned samples with x =0 and 0.16. In these systems, the highest T_c (41 K) was obtained at x=0.16.[2,19] It is worth recalling that the NMR technique is capable of probing a variety of physical properties of superconductors. We also present the results of the resistivity measurement for the parent compound along with the superconducting $CeFeAsO_{1-x}F_x$ sample.

II. EXPERIMENTAL DETAILS

The samples were prepared by the solid-state reaction using high-purity (99.99%) elements of Ce, As (chips), and Fe, Fe_2O_3 (powders). To obtain CeFeAsO and $CeFeAsF_{0.16}O_{0.84}$

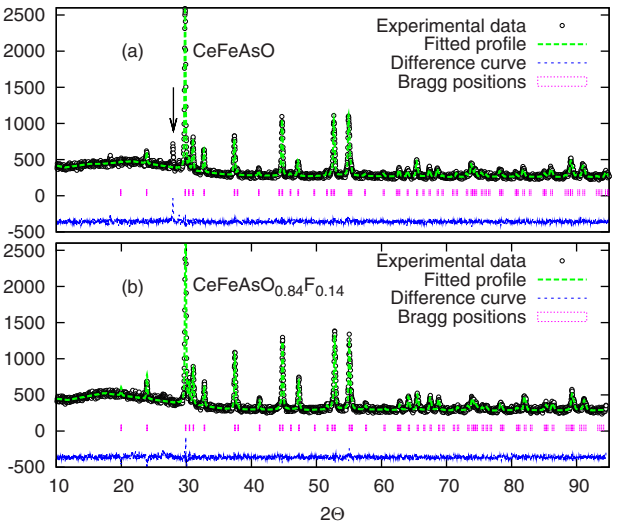

FIG. 1. (Color online) Typical XRD patterns for (a) CeFeAsO and (b) the nominal $CeFeAsF_{0.16}O_{0.84}$ samples; the vertical bars indicate the calculated diffraction peaks. ↓ indicates impurity line.

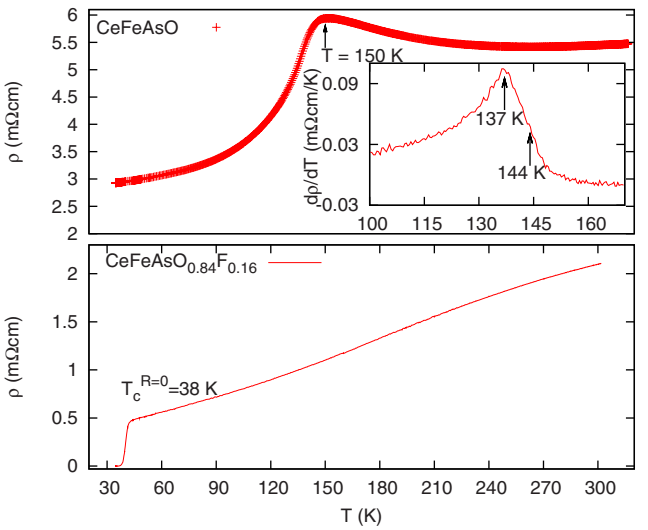

FIG. 2. (Color online) The temperature dependence of resistivity for CeFeAsO and for $CeFeAsO_{0.86}F_{0.16}$. The inset shows the derivative of the resistivity ($d\rho/dT$). Peak corresponding to Fe ordering at 137 K is clearly visible. Arrow at 144 K indicates the structural transition.

samples, we first prepare CeAs and $Ce_{0.9467}As$ by mixing stoichiometric amounts of Ce and As chips inside a glove box filled with inert Ar gas and then sealed in evacuated quartz tubes followed by heat treatment at 600 °C for 12 h and finally fired at 850 °C for 15 h. Each of the pellets was smashed, ground, and finely mixed with stoichiometric amounts of Fe_2O_3 and CeF_3 according to the CeFeAsO and $CeFeAsF_{0.16}O_{0.84}$ formula, respectively. The pressed pellets obtained for each of the compounds were then wrapped with Ta foil and sealed in evacuated quartz tubes. They were then annealed at 1150–1200 °C for 48 h.

Both the samples were characterized using powder x-ray diffraction (XRD) technique with Cu $K\alpha$ radiation at room temperature. Resistivity of CeFeAsO and $CeFeAsF_{0.16}O_{0.84}$ samples were measured using the standard four-probe technique. Electrical contacts were made by conducting silver paste.

The NMR measurements were carried out in a conventional phase-coherent spectrometer at a fixed field of $H_0 = 7.04$ T by changing the frequency step by step and recording the spin-echo intensity by applying a $\pi/2-\tau-\pi/2$ solid echo sequence. The temperature variation studies in the range 3.8–300 K were performed in a continuous flow cryostat with a ITC503 controller (Oxford instruments). The powder sample was aligned in the NMR coil by mixing the fine powders with an epoxy (Epotek-301) and keeping overnight in the magnetic field of 7 T. We attempted to measure the ^{75}As NMR spin-lattice relaxation time, however, because of very short (<5 ms) relaxation time, we were unable to measure it in the whole temperature range.

III. RESULTS AND DISCUSSION

Figure 1 shows the room-temperature XRD patterns for the undoped CeFeAsO and doped $CeFeAsF_{0.16}O_{0.84}$ samples. All the peaks can be indexed on the basis tetragonal ZrCuSiAs-type structure with space group $P4/mmm$. A small impurity peak (shown by ↓) around 102 line is noted only in the undoped sample. The lattice parameters for the undoped and F-doped samples obtained by the profile fit to the respective experimental data are $a=4.000$ Å and $c=8.654$ Å and $a=3.9946$ Å and $c=8.6319$ Å, respectively. Reduction in the cell volume by F doping indicates complete chemical substitution and also consistent with the reported values.

The thermal variation in resistivity of both the undoped as well F-doped samples is shown in Fig. 2. With the decrease in temperature $\rho(T)$ of the undoped sample slowly increases and then below around 148 K it drops steeply without showing any superconducting transition. The room-temperature resistivity value of the undoped sample is larger than that of F-doped sample. The $\rho(T)$ pattern of the undoped sample is quite similar to those reported in *Ln*FeAsO systems exhibiting anomaly in the range 145–150 K.[16,21] Derivative of the resistivity with temperature $d\rho/dT$ clearly shows a pronounced peak at 137 K (inset of Fig. 2) indicating the onset of the long-range magnetic ordering of the Fe spins in CeFeAsO.[19] Moreover, the indication of structural phase transition at 144 K is visible from the change in the slope of the $d\rho/dT$ curve.

We also observed that $\rho(T)$ in $CeFeAsF_{0.16}O_{0.84}$ instead of showing anomaly decreases linearly down to 42 K (T_c^{onset}) and then it drops sharply to zero around 37 K ($T_c^{R=0}$). The superconducting transition width of our F-doped sample is found to be $\Delta T_c = T_c(90\%) - T_c(10\%) = 2.3$ K, implying that the superconducting transition in $CeFeAsF_{0.16}O_{0.84}$ sample is quite sharp compared to that for F-doped LaFeAsO sample.

Figure 3 shows the typical ^{75}As NMR spectra in oriented sample ($H \| ab$) of $CeFeAsO_{0.86}F_{0.16}$ and CeFeAsO taken at 200 K. The spectrum consists of a sharp central peak and two satellites due to the nuclear quadrupolar interaction. A powder pattern typical of the second-order quadrupolar interaction in case of $CeFeAsO_{0.86}F_{0.16}$ is also shown. A comparison of the central transition in case of powder and the aligned

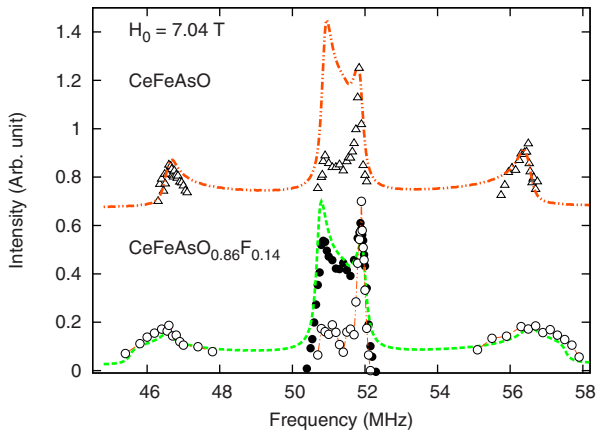

FIG. 3. (Color online) ^{75}As NMR spectra in partially aligned CeFeAsOF (△) and CeFeAsO$_{0.84}$F$_{0.16}$ (○) sample taken at 7.04 T and 200 K. Simulated powder patterns are shown by the dashed lines. Powder pattern of CeFeAsO$_{0.84}$F$_{0.16}$ (●) has also been shown by filled circle.

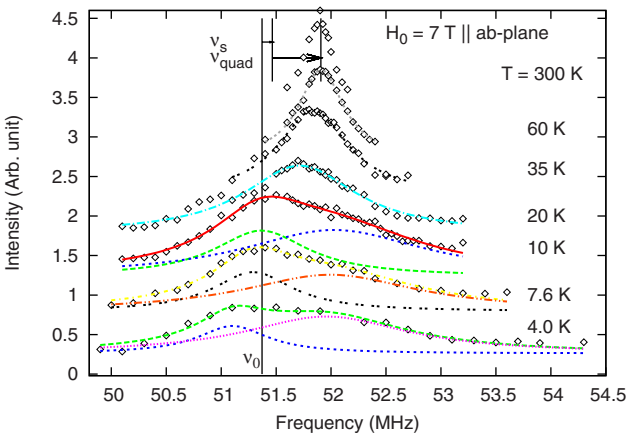

FIG. 4. (Color online) ^{75}As NMR spectra in CeFeAsO$_{0.84}$F$_{0.16}$ at different temperature. ν_0 is the position of the reference frequency. Contribution for ν_s and ν_{quad} for 300 K spectrum has been shown by arrows.

sample indicates that more than 70% of the grains are aligned with $H \perp c$ axis. Simulated powder pattern with $K_{iso}=0.25\% \pm 0.03$, $K_{ax}=-0.016\%$, $K_{an} \sim 0.0$, $\nu_Q = 11.0 \pm 0.2$ MHz, and $\eta=0.09 \pm 0.02$ is also shown. In CeFeAsO, we obtain a smaller $\nu_Q=9.9 \pm 0.2$ MHz and $\eta = 0.02 \pm 0.02$ indicating that the electric field gradient (EFG) is axially symmetric in the undoped sample. This is the general trend for all parent nonsuperconducting compounds.[22]

The resonance frequency of the spectra for the oriented powder ($H \| ab$) is given by $\nu=\nu_0+\nu_s+\nu_{quad}=\nu_0(1+K_{ab}) + 3\nu_Q^2/(16\nu_0)$ for $\eta=0$. The temperature dependence should generally come only from the shift K_{ab}, as ν_{quad} is found to be temperature independent. The magnetic shift arises from the interaction between the As nuclei and the surrounding electrons and can be partitioned into K_s and K_{orb} parts, where K_s arises via a hyperfine coupling to electron spin, and K_{orb} arises from the orbital magnetization induced at the nuclear site. Estimation of K_{orb} is very delicate in this system as K_s is very small in the FeAs system; for example, it is $\sim 0.03-0.04\%$ for the case of ^{75}As Knight shift in LaFeAs(O,F) system.[23] Grafe *et al.*[24] from K_{ab} vs χ and the linear plot of $(T_1T)^{-1/2}$ vs K_{ab}, assuming negligible diamagnetic and Van Vleck contribution to χ_{powder} found $K_{orb} \sim -0.08\%$ who have done ^{75}As NMR in LaFeAsO$_{0.9}$F$_{0.1}$. Ahilan *et al.*[25] quoted $K_{orb} \equiv K_{chem}$ as 0.003% from ^{19}F NMR in a powdered sample of LaFeAsO$_{0.89}$F$_{0.11}$. They, on the other hand, used the relation $1/T_1T$ proportional to K. Imai *et al.*[26] obtained a similar value of 0.0045 % in the oriented sample of LaFeAsO$_{0.9}$F$_{0.1}$ and they have extrapolated this value to find K_{chem} of ^{75}As as about $\leq 0.1\%$. Since we have no χ and $1/T_1$ data for the present sample, we have taken K_{orb} as -0.08% following Ref. 24.

Figure 4 shows the central line of ^{75}As NMR spectra in F-doped oriented sample at some selected temperatures. It is seen that the line remains almost unaltered down to 60 K. Below 60 K, the line starts to broaden along with a gradual shift toward the low-frequency side. The broadening below T_C arises due to the formation of a vortex lattice in the superconducting state. Similar observation was also obtained in PrFeAsO$_{0.89}$F$_{0.11}$.[27] However, the lines can be fitted to the Lorentzian shape down to 20 K. This provides the temperature variation in the peak position (i.e., the total shift) and the linewidth. From the total shift, the contribution due to ν_{quad} and K_{orb} have been subtracted to obtain K_{ab} and has been shown in Fig. 5. K_{ab} for the parent compound has also been estimated in the similar way and shows a small but definite decrement with lowering of temperature, though magnetic susceptibility in the parent compound shows a small increment in the range 140–300 K.[16] Below 140 K, the NMR signal in the parent compound shows appreciable broadening and finally disappears below 138 K; a consequence of the long-range ordering of the Fe moments as indicated in the observed resistivity anomaly at 137 K.

In CeFeAsO$_{0.84}$F$_{0.16}$, the K_{ab} does not show any significant variation in the range 60–300 K. Below 60 K, K_{ab} starts to decrease and the decrement continues below T_c. In other

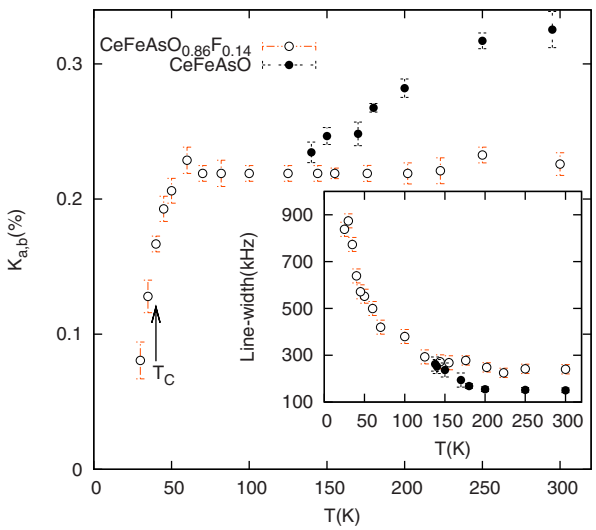

FIG. 5. (Color online) The temperature variation of the ^{75}As Knight shift in CeFeAsO$_{0.84}$F$_{0.16}$ (○) and CeFeAsO (●) with $H \| ab$. K_{orb} was taken as -0.08%. Inset shows variation in linewidth (FWHM).

F-doped *Ln*FeAsO (*Ln*=La and Pr) compounds, the decrement of the shift starts from T_c as a result of the spin-singlet pairing.[24,27]

In both pure and F-doped compounds, in addition to the intrinsic contribution from Fe 3*d* in the FeAs layer to K_{ab} at the As nuclear site, there is a contribution from the dipolar field $H_{\rm dip}$ arising from the *Ln* 4*f*. Therefore, the nature of the temperature dependence of K_{ab} is expected to be similar in both the compounds; but it is not so. The only difference in the magnetic properties of the two compounds is that, in CeFeAsO, Fe 3*d* electrons order antiferromagnetically near 140 K as confirmed from magnetic-susceptibility and Fe Mossbauer studies;[16] whereas, no such ordering occurs in $CeFeAsO_{0.84}F_{0.16}$. Thus it seems that As atom, being situated in between the two Fe atoms, experiences a decrease in K_{ab} (produced by the two Fe atoms situated on both sides), due to the development of the short-range antiferromagnetic correlation above SDW transition. As a result of this Fe ordering, the contribution to K_{ab} at the As site due to Fe 3*d* electrons overcomes that due to Ce 4*f* electrons ($K_{\rm dip}$) in CeFeAsO compared to that in the F-doped compound. Since the separation of $K_{\rm dip}$ from K_{ab} is not an easy task, the decrement of K_{ab} in $CeFeAsO_{0.84}F_{0.16}$ below 60 K, which is higher than T_c=41 K, cannot be ascribed due to the only spin-singlet Cooper pairing state.

Below 20 K, the resonance line shape becomes highly asymmetric toward the high-frequency side with the peak shifted toward the low-frequency side with respect to the diamagnetic reference. To find the different contribution, we have fitted the spectra considering two Lorentzian lines. These two lines seem to be arising from the presence of both superconducting state and the normal state of the material. The peak corresponding to the superconducting state shifted toward the low frequency corresponding to the ^{75}As resonance in diamagnetic reference. This negative shift increases continuously until 4.0 K. Since for a singlet $d_{x^2-y^2}$ wave superconductor, the local density of states of electrons is suppressed away from the vortex cores but recovers at the cores[28] then it is expected that a Redfield[29] pattern of the spin shift $^{SC}K_{c,\rm spin}(\nu)$ due to the electron density of states affects the NMR spectrum. However, the observed negative shift indicates that a Redfield pattern of a superconducting diamagnetic shift $^{SC}K_{\rm dia}$ is the predominant distribution over that expected pattern due to the spin shift. In general, the peak frequency of the spectrum can be assigned to the saddle point in the field distribution of vortices, the highest frequency spectrum arises from the nuclei close to the vortex core, and the lowest frequency edge to the minimum field position almost away from the vortex core. In the present case, the lowest-frequency edge is not discernible. Here we would not attempt for the detail Redfield fitting to find the London penetration depth λ; nevertheless, from the second moment and/or the linewidth [full width at half maximum (FWHM)] of the line shape we can estimate a value for λ providing important information on the vortex lattice. It may be mentioned that formation of a vortex lattice in the superconducting state has already been mentioned in case of $LaFeAsO_{0.89}F_{0.11}$ (Ref. 25) and $PrFeAsO_{0.89}F_{0.11}$.[27]

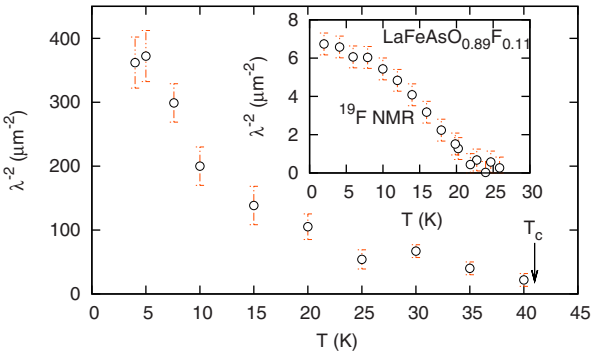

FIG. 6. (Color online) The temperature variation of λ^{-2} in case of $CeFeAsO_{0.84}F_{0.16}$ (see text for estimation). Inset shows the same in $LaFeAsO_{0.84}F_{0.16}$ taken from Ref. 25.

Since these iron pnictide superconductors are of extreme-type II, ($B_{c1}\sim 0.005$ T and $B_{c2}\sim 60$ T), we have large range of applied fields $B_{\rm appl}<B_{c2}/4$, where simple London picture applies.[30] We have estimated the London penetration depth λ from the line broadening which arises because superconducting vortices induce a distribution of the local magnetic field $B_{\rm local}$ inside the sample as mentioned earlier. In the present case, the reduced field $b\equiv B_{\rm appl}/B_{c2}=0.12<1$, following the calculation of Ref. 30, we have $\Delta B_{\rm local}\sim 0.117\,4\phi_0/\lambda^2$, where $\phi_0=2.0678\times 10^{-15}$ Tm^2. We have deduced $\Delta B_{\rm local}$ below T_C by subtracting the background linewidth (FWHM) obtained at 60 K. Figure 6 shows the variation of λ^{-2} with temperature. It is seen that λ^{-2} continues to grow down to 4 K, if $CeFeAsO_{0.84}F_{0.16}$ was a conventional *s*-wave superconductor, λ^{-2} would saturate below $T\sim 0.4T_c=16$ K. Though this nature is similar[25] (as shown in the inset of Fig. 6) to that found in case of $LaFeAsO_{0.89}F_{0.11}$, the value of λ^{-2} in the present case is considerably higher, indicating a smaller penetration depth. However, we would not attempt to estimate λ at $T=0$ limit as was done in Ref. 25 since our samples are not fully aligned and moreover As being a quadrupolar nuclei (having a large ν_Q), quadrupolar broadening may affect the line as well. However, the short value of λ is consistent with the observation of the Redfield pattern at low temperature in the present sample $CeFeAsO_{0.84}F_{0.16}$.

IV. SUMMARY

To summarize, we have reported the resistivity and ^{75}As NMR results in superconducting $CeFeAsO_{0.84}F_{0.16}$ and its parent compound CeFeAsO. The derivative of the resistivity with temperature and ^{75}As NMR in CeFeAsO clearly show a signature of the onset of long-range magnetic ordering. The resistivity in $CeFeAsO_{0.84}F_{0.16}$ drops sharply at 41 K and becomes zero at 38 K. Analyzing the ^{75}As NMR spectra in $CeFeAsO_{0.84}F_{0.16}$ and CeFeAsO, we obtained the value of quadrupolar splitting frequency ν_Q=11.0 and 9.9(±0.2) MHz and asymmetry parameter η=0.09 and 0.02, respectively. The shift K_{ab} in the oriented ($H\|ab$)$CeFeAsO_{0.84}F_{0.16}$ sample starts to decrease from 60 K (above T_c). To clarify this point, we need to measure χ and $1/T_1$ to obtain correct estimation of $K_{\rm orb}$, which may be delicate in this sample. Nature of the temperature dependence of

the Knight shift has been discussed considering different contributions to the local magnetic field at the As site. Below 30 K, the NMR line broadens asymmetrically due to the formation of vortex lattice and the NMR spectra at 4–10 K resemble the Redfield pattern indicating a small value of London penetration depth λ. To have accurate quantitative estimation of $\lambda(0)$, we need a fully aligned sample or a single crystal of high purity.

*amitabha.ghoshray@saha.ac.in

[1] Y. Kamihara, T. Watanabe, M. Hirano, and H. Hosono, J. Am. Chem. Soc. **130**, 3296 (2008).
[2] G. F. Chen, Z. Li, D. Wu, G. Li, W. Z. Hu, J. Dong, P. Zheng, J. L. Luo, and N. L. Wang, Phys. Rev. Lett. **100**, 247002 (2008).
[3] X. H. Chen, T. Wu, G. Wu, R. H. Liu, H. Chen, and D. F. Fang, Nature (London) **453**, 761 (2008).
[4] Z. A. Ren, J. Yang, W. Lu, W. Yi, G.-C. Che, X.-L. Dong, L.-L. Sun, and Z.-X. Zhao, Mater. Res. Innovations **12**, 105 (2008).
[5] J. Yang, Z.-C. Li, W. Lu, W. Yi, X.-L. Shen, Z.-A. Ren, G.-C. Che, X.-L. Dong, L.-L. Sun, F. Zhou, and Z.-X. Zhao, Supercond. Sci. Technol. **21**, 082001 (2008).
[6] J. G. Bos, G. B. S. Penny, J. A. Rodgers, D. A. Sokolov, A. D. Huxley, and J. P. Attfield, Chem. Commun. (Cambridge) **2008**, 3634.
[7] Z.-A. Ren, W. Lu, J. Yang, W. Yi, X.-L. Shen, Z.-C. Li, G.-C. Che, X.-L. Dong, L.-L. Sun, F. Zhou, and Z.-X. Zhao, Chin. Phys. Lett. **25**, 2215 (2008).
[8] H. Kito, H. Eisaki, and A. Iyo, J. Phys. Soc. Jpn. **77**, 063707 (2008).
[9] M. Rotter, M. Tegel, D. Johrendt, I. Schellenberg, W. Hermes, and R. Pöttgen, Phys. Rev. B **78**, 020503(R) (2008).
[10] F. Bondino, E. Magnano, M. Malvestuto, F. Parmigiani, M. A. McGuire, A. S. Sefat, B. C. Sales, R. Jin, D. Mandrus, E. W. Plummer, D. J. Singh, and N. Mannella, Phys. Rev. Lett. **101**, 267001 (2008).
[11] C. de la Cruz, Q. Huang, J. W. Lynn, J. Li, W. Ratcliff, J. L. Zarestky, H. A. Mook, G. F. Chen, J. L. Luo, N. L. Wang, and P. C. Dai, Nature (London) **453**, 899 (2008).
[12] T. Nomura, S. W. Kim, Y. Kamihara, M. Hirano, P. V. Sushko, K. Kato, M. Takata, A. L. Shluger, and H. Hosono, Supercond. Sci. Technol. **21**, 125028 (2008).
[13] Y. Kohama, Y. Kamihara, M. Hirano, H. Kawaji, T. Atake, and H. Hosono, Phys. Rev. B **78**, 020512(R) (2008).
[14] S. Kitao, Y. Kobayashi, S. Higashitaniguchi, M. Saito, Y. Kamihara, M. Hirano, T. Mitsui, H. Hosono, and M. Seto, J. Phys. Soc. Jpn. **77**, 103706 (2008).
[15] Y. Nakai, K. Ishida, Y. Kamihara, M. Hirano, and H. Hosono, J. Phys. Soc. Jpn. **77**, 073701 (2008).
[16] M. A. McGuire, R. P. Hermann, A. S. Sefat, B. C. Sales, R. Jin, D. Mandrus, F. Grandjean, and G. J. Long, New J. Phys. **11**, 025011 (2009).
[17] J. Zhao, Q. Huang, C. de la Cruz, J. W. Lynn, M. D. Lumsden, Z. A. Ren, J. Yang, X. Shen, X. Dong, Z. Zhao, and P. Dai, Phys. Rev. B **78**, 132504 (2008).
[18] S. Chi, D. T. Adroja, T. Guidi, R. Bewley, S. Li, J. Zhao, J. W. Lynn, C. M. Brown, Y. Qiu, G. F. Chen, J. L. Lou, N. L. Wang, and P. Dai, Phys. Rev. Lett. **101**, 217002 (2008).
[19] J. Zhao, Q. Huang, C. Delacruz, S. Li, J. Lynn, Y. Chen, M. Green, G. Chen, G. Li, Z. Li, J. Luo, N. Wang, and P. Dai, Nature Mater. **7**, 953 (2008).
[20] Y. Chen, J. W. Lynn, J. Li, G. Li, G. F. Chen, J. L. Luo, N. L. Wang, P. Dai, C. dela Cruz, and H. A. Mook, Phys. Rev. B **78**, 064515 (2008).
[21] M. A. McGuire, A. D. Christianson, A. S. Sefat, B. C. Sales, M. D. Lumsden, R. Jin, E. A. Payzant, D. Mandrus, Y. Luan, V. Keppens, V. Varadarajan, J. W. Brill, R. P. Hermann, M. T. Sougrati, F. Grandjean, and G. J. Long, Phys. Rev. B **78**, 094517 (2008).
[22] H. Mukuda, N. Terasaki, H. Kinouchi, M. Yashima, Y. Kitaoka, S. Suzuki, S. Miyasaka, S. Tajima, K. Miyazawa, P. Shirage, H. Kito, H. Eisaki, and A. Iyo, J. Phys. Soc. Jpn. **77**, 093704 (2008).
[23] A. Kawabata, S. C. Lee, T. Moyoshi, Y. Kobayashi, and M. Sato, and J. Phys. Soc. Jpn. **77**, 103704 (2008).
[24] H.-J. Grafe, D. Paar, G. Lang, N. J. Curro, G. Behr, J. Werner, J. Hamann-Borrero, C. Hess, N. Leps, R. Klingeler, and B. Büchner, Phys. Rev. Lett. **101**, 047003 (2008).
[25] K. Ahilan, F. L. Ning, T. Imai, A. S. Sefat, R. Jin, M. A. McGuire, B. C. Sales, and D. Mandrus, Phys. Rev. B **78**, 100501(R) (2008).
[26] T. Imai, K. Ahilan, F. Ning, M. A. McGuire, A. S. Sefat, R. Jin, B. C. Sales, and D. Mandrus, J. Phys. Soc. Jpn. **77**, 47 (2008).
[27] K. Matano, Z. A. Ren, X. L. Dong, L. L. Sun, Z. X. Zhao, and G.-Q. Zheng, EPL **83**, 57001 (2008).
[28] M. Takigawa, M. Ichioka, and K. Machida, J. Phys. Soc. Jpn. **69**, 3943 (2000).
[29] A. G. Redfield, Phys. Rev. **162**, 367 (1967).
[30] E. H. Brandt, Phys. Rev. B **37**, 2349 (1988).